Plasma Compression using Rotating Electric Fields – the Strong Drive Regime

J. R. Danielson and C. M. Surko

Department of Physics, University of California, San Diego, La Jolla, CA 92093

Abstract. The rotating wall technique has proven to be an excellent method to create high-density, single-component plasmas in Penning-Malmberg traps. It has become useful, and sometimes critical, for applications such as antihydrogen production and the tailoring of ion crystals and positron beams. Azimuthally phased rf fields apply a torque that injects angular momentum and produces radial plasma compression as it spins the plasma up. Recently, we discovered a new "strong-drive" regime in which plasmas can be compressed until the E x B rotation frequency, f_E (where $f_E \propto n$, the plasma density) approaches the applied frequency, f_{RW}. We review here highlights of a recently published study of this regime [Danielson, *et al.*, Phys. Plasmas **13**, 055706 (2006)]. Good compression is achieved over a broad range of RW frequencies without the need to tune to a plasma mode. Setting the plasma density can be done simply and reliably by tuning f_{RW}. Characteristics of this strong-drive regime and the resulting high-density steady states are discussed.

Keywords: Nonneutral plasmas, Penning-Malmberg traps, antimatter plasmas
PACS: 52.27.Jt, 52.25.Xz, 52.25.Fi, 52.25Kn

INTRODUCTION

There are many uses of trapped single-component plasmas such as in atomic clocks, tailoring positron beams for materials characterization, and the production of low-energy antihydrogen [1, 2]. Beyond the applications, these plasmas are interesting in their own right, due in no small part to the fact that they can be prepared and maintained in thermal equilibrium states. Consequently it is important to understand the range of accessible plasma parameters, including the limits on plasma temperature and density, and the factors that limit plasma confinement. Recently we reported a study of torque-balanced steady states of electron plasmas using cyclotron cooling to mitigate plasma heating and a rotating electric field [i.e., the so-called 'rotating wall' (RW) technique] for radial compression and the mitigation of outward transport [3, 4]. In this paper, we review these experiments and identify unique characteristics of this novel, strong-drive regime of RW compression.

In an ideal, cylindrically symmetric Penning-Malmberg trap, there are no asymmetries to break the conservation of angular momentum. In practice, plasmas in these devices expand due to the torques arising from small trap asymmetries, either electric or magnetic in origin. While this asymmetry-driven expansion is present in all traps, the particular details vary widely depending on the plasma parameters and the nature of the trap asymmetries [5-7].

CP862, *Non-Neutral Plasma Physics VI, Workshop on Non-Neutral Plasmas 2006,*
edited by M. Drewsen, U. Uggerhøj, and H. Knudsen

The intimate relationship between the angular momentum and plasma radius has lead to the development of a very effective method to radially compress magnetized single-component plasmas. Namely, the application of a torque increases the angular momentum, resulting in a decrease in the radial extent of the plasma. This can be accomplished conveniently and effectively using a rotating (RW) electric field or, for ion plasmas, using the absorption and re-emission of laser light to inject angular momentum [8]. The effectiveness of this technique depends upon the efficiency of coupling of the external RW torque to the plasma and the nature of the inherent drag torque [4]. Since the external agent used to apply the torque does work on the plasma and heats it, an efficient plasma cooling mechanism is required for good compression.

Rotating-wall fields have been used in a variety of situations, including large ion clouds [9], small ion crystals [10, 11], electron plasmas [12, 13], and positron plasmas [14-17]. Much of this work was done in a regime in which the RW fields couple to Trivelpiece-Gould modes in the plasma (e.g., Ref. [13]). The compression experiments reported here are done on electron plasmas in a "low-slip" regime in which the plasma rotation frequency is close to the RW drive frequency – a regime in which coupling to plasma modes is extremely unlikely. In the studies reported here, strong cyclotron cooling combined with the weak torque necessary to maintain the compressed plasma results in states weakly perturbed from thermal equilibria. This raises the possibility that the resulting torque-balanced steady states can be described quantitatively using equilibrium statistical mechanics [18], which is an idea that we are currently exploring [19].

The remainder of this paper is organized as follows. We describe the experimental apparatus, the methods used to measure the density and temperature, and details of a typical compression experiment. We then describe the results of these experiments, and in particular, identify the principal factors relevant to the manipulation and control of trapped plasmas. We conclude by summarizing key results and discussing briefly possible directions for future research.

DESCRIPTION OF THE EXPERIMENTS

The experiments were performed in a cylindrical Penning-Malmberg trap, shown schematically in Fig. 1 [4]. Plasmas are confined radially by a 4.8 T magnetic field, with axial confinement provided by voltages (typically −100 V) applied to the end electrodes. The wall diameter is 2.54 cm, and the plasma length, L_p, can be varied in the range $5 < L_p < 25$ cm by using different electrode configurations. Electron plasmas

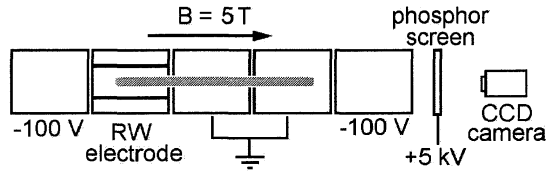

Figure 1. Schematic diagram of the experiment (not to scale; not all electrodes are shown).

are injected using a standard electron gun, with initial plasma radii $R_p \sim 1$ - 2 mm, and particle numbers, N, in the range $10^8 < N < 10^9$. The data presented here correspond to $N = 3\text{x}10^8$. The effect of N on plasma confinement and dynamics over a broader range of N is currently under investigation.

Rotating electric fields are applied to the plasma using a special-purpose, four-phase rf generator attached to a four-segment electrode. Each segment extends 90° azimuthally and 2.54 cm axially; combined, they produce a radial electric field with azimuthal mode number $m_\theta = 1$ rotating in the same direction as the plasma. While the rf circuit can operate from 0.1 to 80 MHz, studies thus far have been limited to $f_{RW} <$ 15 MHz. While the origin of this limitation is not fully understood, it appears likely that it is related to electronic resonances associated with the electrode structure and associated circuitry, rather than to an intrinsic plasma effect.

The data presented here correspond to the RW electrode located near one end of the plasma column, as shown in Fig. 1, but good confinement and compression have also been achieved with the RW at other locations. Theoretically, an $m_\theta = 1$ rf dipole field applied over the entire plasma can drive no torque [18]. Although not studied in detail, we find that good compression can be achieved as long as the axial extent of the RW electrode is less than half the plasma length.

The trap is operated in "inject-manipulate-dump" cycles that exhibit very good shot-to-shot reproducibility, typically $\delta N/N \sim 1\%$, where N is the particle number. Density profiles are measured by accelerating the dumped plasmas onto a phosphor screen biased to +5 kV and imaged with a CCD camera. The profile is obtained by radially averaging the images about the center of the plasma. Alternatively, the screen can be attached to a charge-to-voltage amplifier for measuring the total charge, $Q = Ne$.

The parallel plasma temperature, $T_\parallel$, is measured by a standard evaporation technique [20]. For the plasmas studied here, the perpendicular-to-parallel equilibration rate is rapid, $\nu_{\perp\parallel} > 10^3\ s^{-1}$, so $T_\perp \sim T_\parallel = T$ [21]. Heat transport is also rapid with the thermal relaxation time $\tau < 10$ ms [22], and so we assume the temperature is independent of radius. The plasma cools by cyclotron radiation in the 4.8 T magnetic field at a measured rate $\Gamma_c \sim 5.9\ s^{-1}$ [21], which is fast compared to the compression and expansion rates. Thus, in most cases, the plasmas remain relatively cool even in the presence of strong RW fields.

After the plasma is injected into the trap, the RW field is turned on *at a fixed frequency* f_{RW} and amplitude V_{RW}. The evolution of the plasma is studied by repeating the experiment for different hold times. This is in contrast to previous experiments that utilized frequency ramps [12]. The time-evolution of n and T during RW compression is shown in Fig. 2. Here the central density n_0 is plotted as a function of RW time, where the RW is turned on at t = 0 with $f_{RW} = 4$ MHz and $V_{RW} = 1.0$ V. There are two density data points at each time. Typically they differ by < 1%, providing a demonstration of the robust compression and reproducibility of the experiment. Each temperature data point is the average of four measurements, and the error bars represent the typical variation of these data.

Figure 2 shows the evolution of a typical plasma in what we identify below as the "strong-drive" regime. The plasma density rises exponentially to a steady-state value,

corresponding to a rotation frequency that is very close to the applied frequency. The temperature rises rapidly to about 3 eV in the first 20 ms, levels off, and then drops at an exponential rate comparable to that of the density rise. We note that the rate of temperature evolution [i.e., $(1/T)dT/dt \sim 1.0\ s^{-1}$] is much slower than the cyclotron cooling rate, indicating that the heating from the RW and the cyclotron cooling are very nearly balanced during plasma compression. Also, the cooling rate gets faster as the density increases as a result of the fact that the heating rate decreases as f_E approaches f_{RW}.

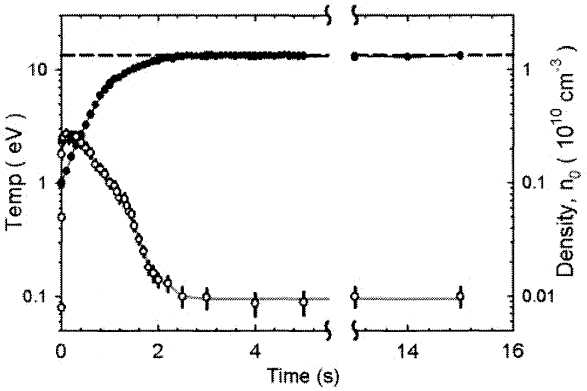

Figure 2. Central density, n_0 (●) and temperature, T (○), as a function of time after the RW is applied, for f_{RW}= 4 MHz, V_{RW} = 1.3 V, and $L_p \sim 14$ cm. The dashed line indicates the density for no-slip condition, $f_E = f_{RW}$).

STRONG-DRIVE COMPRESSION

A series of experiments were conducted to investigate the range of achievable plasma parameters accessible utilizing strong RW drive. The main results, published previously in Refs. [3, 4], are shown in Figs. 3 - 6. The behavior illustrated in these figures is typical of "strong-drive" RW compression, a key signature of which is the tendency for the plasma to reach a low-slip steady state in which f_E is very close to f_{RW}.

The transition to this new regime is illustrated in Fig. 3. Shown in this figure is a series of compression experiments conducted at fixed frequency for different values of the drive amplitude, V_{RW}. For $V_{RW} < 0.7$ V, the plasma is compressed to a limiting density of about 5×10^9 cm^{-3}. However, at $V_{RW} = 0.7$ V, there is a bifurcation to a new, high-density regime. Above this RW drive amplitude, the plasma always compresses to a much higher density with n approaching 2×10^{10} cm^{-3} for the chosen value of f_{RW}. For values of $V_{RW} > 0.7$ V, the compression rate increases, but this only weakly affects the final steady state in which $f_E \approx f_{RW}$.

For fixed large-amplitude drive, plasma compression and high-density steady states are achieved for a range of drive frequencies. This is illustrated in Fig. 4, where the density evolution is shown for drive frequencies between 0 and 10 MHz, with V_{RW}

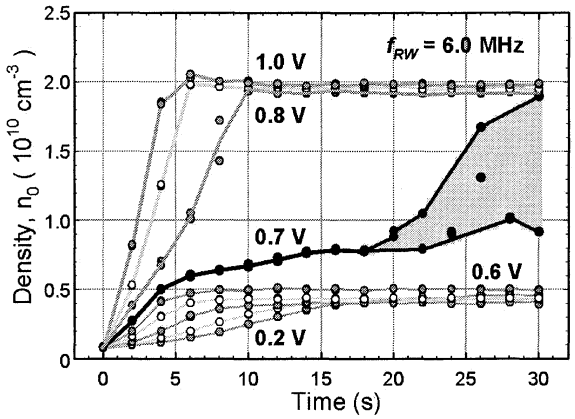

Figure 3. Time evolution of plasma density for different drive amplitudes, V_{RW}, at f_{RW} = 6 MHz. The data sets shown correspond to successive increases of V_{RW} by 0.1 V. Of particular note is the bifurcation from the weak-drive regime to the strong-drive regime and the resulting saturation of the density increase that occurs at V_{RW} = 0.7 V. Reprinted from Ref. [4].

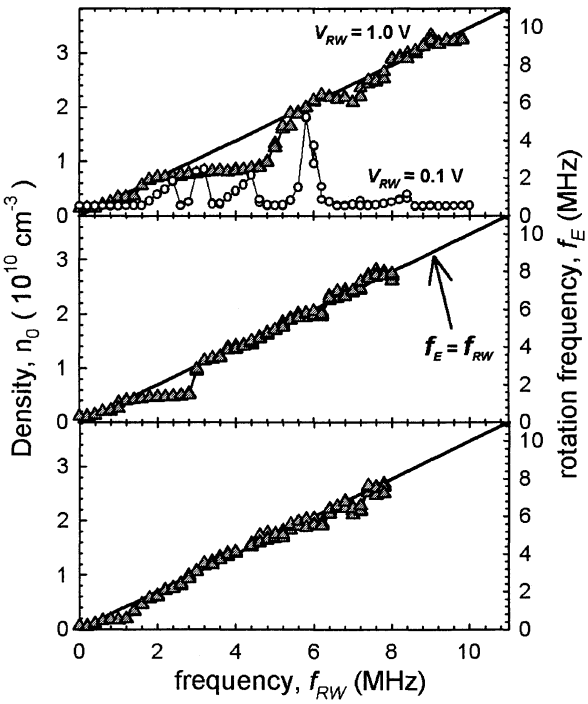

Figure 4. Steady-state density *vs* f_{RW} for plasma lengths (from top to bottom) of 10, 14, and 24 cm, for values of V_{RW} = 1.0 V (▲) (the strong drive regime), and 0.1 V (○) (weak drive). The solid lines show the no slip condition, $f_{RW} = f_E$. Reprinted from Ref. [4].

= 1.0 V, for three different plasma lengths. As the frequency increases, the steady-state density also increases. Note that the vertical scale is given in terms of both density and the plasma rotation frequency, f_E. In the top panel of this plot, data are shown for two values of drive amplitude, V_{RW} = 1.0 V and 0.1 V, for a plasma length of 10 cm. As expected, in the weak-drive case, significant compression is observed only near discrete frequencies, likely due to strong coupling to plasma modes, similar to the behavior described in Ref. [12].

The behavior at large drive amplitude is qualitatively different. This is illustrated in Fig. 4, where the data show large ranges of f_{RW} for which strong plasma compression is observed. Note that the plasma rotation frequency, f_E approaches the RW frequency (i.e., solid lines in Fig. 4). This close matching of the plasma rotation to the drive frequency is commonly called the condition of "low-slip," i.e., $\Delta f = f_{RW} - f_E << f_{RW}$ [9]. The RW heating power delivered to the plasma is proportional to this slip. Hence low slip implies low power and relatively low amounts of heating, as illustrated, for example, by the steady-state portion of data shown in Fig. 2. The rates of thermal and momentum transport are large compared to those for compression and cyclotron cooling, and so the plasmas remain close to thermal equilibria. This is consistent with the measured radial plasma profiles that closely approximate constant-density profiles characteristic of the expected rigid-rotor, thermal equilibrium states [4].

For the two longer length plasmas shown in Fig 4, the lack of data above 8 MHz indicates that no steady-state density was achieved. At these frequencies, the initial plasma temperature rise is greater than 5 eV, causing ionization of the background gas. This tends to drive an ion-resonance instability [23] that results in a significant loss of plasma.

It is important to clarify that strong drive does not imply that a large torque is required in the high-density, low-slip state. In fact, the torque and associated plasma heating are relatively small in the low-slip state. Rather, strong drive refers to the observation that there is a relatively large minimum torque required *to access* this high density, low-slip state and during the early phases of plasma compression. Finally, we note that the "steps" in the strong-drive data shown in Fig. 4 are due to coupling of the plasma to static field asymmetries, as discussed in more detail in Ref. [4].

Shown in Fig. 5 is the dynamic response of the plasma when subject to a change in the drive amplitude. Here the density evolution is shown for a plasma that was initially compressed with V_{RW} = 1.0 V for t = 15 s, then the drive amplitude was decreased to 0.5, 0.2, and 0 V. As shown by the gray squares, a decrease in amplitude by a factor of two causes the density to decrease by $\leq$ 5%. Note (e.g., Fig. 3) that this amplitude is, in fact, below the transition amplitude corresponding to the strong-drive regime. In particular, the application of this small of an initial drive amplitude to a low-density plasma *would not* compress it to the high density shown in Fig. 5. As shown by the gray circles in Fig. 5, even a factor of five smaller drive amplitude is able to maintain the compressed plasma state with a density drop of only ~ 20%. Thus the plasma exhibits very significant hysteresis as a function of the applied RW amplitude. This hysteresis is a key distinguishing feature of the transition between the strong- and weak-drive compression states.

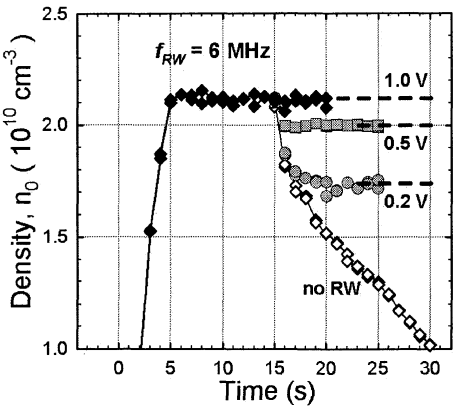

Figure 5. Change in steady-state density in response to changes in V_{RW} for f_{RW} = 6 MHz. The density scale has been expanded to emphasize the changes in density. Note the relative insensitivity of the density to changes in V_{RW}; a factor of two drop in V_{RW} only caused a 5% drop in the density. Reprinted from Ref. [4].

The evolution of the plasma in response to a decrease in f_{RW} is investigated in Fig. 6 for a plasma that was initially compressed with f_{RW} = 8 MHz and V_{RW} = 1.0 V. The resulting evolution when the rotating wall is turned off is also shown for comparison. For decreases to final values f_{RW} < 5 MHz, the rate at which the plasma achieves a new equilibrium is considerably faster than the plasma expansion rate. This indicates that, for these frequency changes, the RW torque is considerably larger than the steady-state torque. These results are consistent with our current theoretical model of this process [19], which predicts that the torque is proportional to the slip, Δf, i.e., the torque is large immediately following the frequency change, but decreases as the plasma approaches the new steady state.

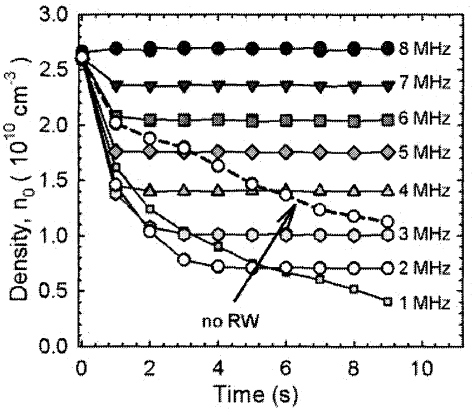

Figure 6. Evolution to a new equilibrium in response to a rapid decrease in f_{RW} from an initial value of 8 MHz. The decrease in density produced by turning off the RW is also shown. Reprinted from Ref. [4].

In general, the strong-drive regime is characterized by relatively rapid RW compression as compared to the rate of the plasma expansion in the absence of the drive. In this regime, the density increases until there is only a fractionally small difference between f_{RW} and f_E. For example, from the data in Fig. 4, for $L_p \sim 14$ cm, $f_{RW} = 6$ MHz, and $\Delta f = f_{RW} - f_E < 0.15$ MHz, corresponding to a fractional slip, $\Delta f/f <$ 3%. This is typical of the small values of slip in the strong-drive regime.

Changing the drive frequency, either up (as in Fig. 6) or down, causes a rapid change to a new equilibrium determined by the final drive frequency [4]. This has important positive implications for the utility of this regime in controlling the plasma parameters. In particular, for the relatively long, cylindrical plasmas studied here, setting the applied frequency in the low slip regime fixes the plasma density that can be adjusted easily by setting f_{RW} while maintaining an approximately constant plasma length.

One application in which this procedure would be useful is the production of antihydrogen from trapped positron and antiproton plasmas. The antihydrogen production rate is dependent on both the plasma density and temperature. The ATHENA group has measured the production *vs* time, by cycling plasma heating on and off, thereby studying the dependence of the production on positron plasma temperature [24]. We note that one could use RW plasma compression in the strong-drive regime to cycle the positron plasma *density* in time by changing f_{RW} (e.g., from 4 and 8 MHz) and thus study the dependence of the antihydrogen production rate on positron density. For example, for the three-body recombination mechanism the factor of two change in density would be expected to produce a factor of four change in the production rate.

SUMMARY AND CONCLUDING REMARKS

In this paper we have presented an overview of recent results in a new "strong-drive" regime of radial compression of single-component plasmas using rotating electric fields and strong cyclotron cooling. The fact that coupling of the fields to plasma modes is not required provides a great simplification in many practical applications. The limiting density corresponds to a "low-slip" condition in which the plasma rotation frequency is very close to the applied RW frequency. Once in the high-density state, only a weak dependence on the drive amplitude is observed demonstrating the hysteresis associated with this bifurcation to the strong drive regime. In this regime, changes in the applied frequency cause a rapid evolution to a new equilibrium with the final density set by the final RW frequency. This provides a convenient and robust method *to control* plasma density.

One important, but as yet unanswered, question is the maximum density that can be achieved using this technique. The present limit on RW frequency (and hence plasma density) appears to be due to extrinsic resonances in the RW electrical circuit. In principle, plasma heating could also be a factor in limiting the maximum achievable density. However, since the observed outward transport, Γ, does not increase rapidly with density in the low-slip regime studied here [4], heating will likely not be a limiting factor, as it would be at lower densities where $\Gamma \sim n^2$ [4, 25].

The robust, virtually ubiquitous, nature of the observed compression indicates that a relatively simple model of the RW torque should be possible, and work along these lines is in progress [19]. In particular, we are seeking to understand the nature of the torque as a function of RW drive voltage and slip frequency by perturbing the system about the low-slip steady state. From a theoretical perspective, and in the language of nonlinear dynamics, the present working hypothesis is that both the weak-drive (high-slip) and the strong-drive (low-slip) states are stable fixed points for some range of parameters. Above a certain RW drive amplitude and with strong cooling, the weak-drive fixed point becomes unstable, and the system is then attracted to the low-slip, high-density fixed point.

The fact that the resulting high-density, steady-state plasmas have profiles close to that expected in thermal equilibrium indicates that the thermodynamic equations for a single-component plasma will likely be useful in understanding the coupling between density, temperature, and torque [18]. If so, the coupled evolution equations for the plasma temperature and density could potentially be used to describe in detail the evolution of the plasma during the transition between the high-slip and low-slip steady states.

The new RW compression regime reported here can be expected to be of considerable practical importance in tailoring antimatter plasmas and beams for a variety of applications, including the creation of Bose-condensed gases of positronium atoms, the formation and trapping of antihydrogen, and the creation of positron beams for atomic physics and materials studies. Recently, we proposed a novel design of *multicell* Penning-Malmberg trap for long-term storage of large numbers of positrons (e.g., $N \geq 10^{12}$) [25, 26]. In this device, the antiparticles will be stored in numerous, separate plasma cells, shielded from one another by copper electrodes, and placed in a common magnetic field and vacuum system. The electrodes screen out the plasma space charge, reducing the required confinement voltages. The low-slip regime of RW operation described here is ideally suited for compressing and confining plasmas in such a device, since careful tuning of the RW frequency is not required. This, in turn, reduces greatly the need for active control of the individual cells, thereby providing considerable simplification in the design of such a trap.

ACKNOWLEDGEMENTS

We thank M. Anderson and T. O'Neil for helpful discussions and E. A. Jerzewski for expert technical assistance. This work was supported by NSF grant PHY 03-54653.

REFERENCES

1. T. M. O'Neil, *Physics Today* **52**, 24, (1998).
2. C. M. Surko and R. G. Greaves, *Phys. Plasmas* **11**, 2333, (2004).
3. J. R. Danielson and C. M. Surko, *Phys. Rev. Lett.* **95**, 035001, (2005).
4. J. R. Danielson and C. M. Surko, *Phys. Plasmas* **13**, 055706, (2006).
5. J. M. Kriesel and C. F. Driscoll, *Phys. Rev. Lett.* **85**, 2510, (2000).
6. J. Notte, J. F. R. Chu, and J. S. Wurtele, *Phys. Rev. Lett.* **70**, 3900, (1993).
7. A. A. Kabantsev, J. H. Yu, R. B. Lynch, *et al.*, *Phys. Plasmas* **10**, 1628, (2003).

8. J. J. Bollinger, D. J. Wineland, and D. H. E. Dubin, *Physics of Plasmas* **1**, 1403, (1994).
9. X. P. Huang, F. Anderegg, E. M. Hollmann, *et al.*, *Phys. Rev. Lett.* **78**, 875, (1997).
10. X. P. Huang, J. J. Bollinger, T. B. Mitchel, *et al.*, *Phys. Rev. Lett.* **80**, 73, (1998).
11. X. P. Huang, R. L. S. J. J. Bollinger, and R. C. Davidson, T. B. Mitchell, *et al.*, *Phys. Plasmas* **5**, 1656, (1998).
12. F. Anderegg, E. M. Hollmann, and C. F. Driscoll, *Phys. Rev. Lett.* **81**, 4875, (1998).
13. E. M. Hollmann, F. Anderegg, and C. F. Driscoll, *Phys. Plasmas* **7**, 2776, (2000).
14. R. G. Greaves and C. M. Surko, *Phys. Rev. Lett.* **85**, 1883, (2000).
15. R. G. Greaves and C. M. Surko, *Phys. Plasmas* **8**, 1879, (2001).
16. D. P. van der Werf, M. Amoretti, G. Bonomi, *et al.*, *Non-Neutral Plasma Physics V*, edited by M. Schauer, T. Mitchell and R. Nebel (American Institute of Physics Press, 2003), 172, (2003).
17. L. V. Jorgensen, M. Amoretti, G. Bonomi, *et al.*, *Phys. Rev. Lett.* **95**, 025002, (2005).
18. D. H. E. Dubin and T. M. O'Neil, *Rev. of Mod. Phys.* **71**, 87, (1999).
19. J. R. Danielson, C. M. Surko, M. W. Anderson, *et al.*, *Bull. Am. Phys. Soc.*, in press, (2006).
20. D. L. Eggleston, C. F. Driscoll, B. R. Beck, *et al.*, *Phys. Fluids B* **4**, 3432, (1992).
21. B. R. Beck, J. Fajans, and J. H. Malmberg, *Phys. Plasmas* **3**, 1250, (1996).
22. E. M. Hollmann, F. Anderegg, and C. F. Driscoll, *Phys. Plasmas* **7**, 1767, (2000).
23. J. Fajans, *Phys. Plasmas* **5**, 3127, (1993).
24. M. Amoretti, C. Amsler, G. Bonomi, *et al.*, *Nature* **419**, 456, (2002).
25. C. M. Surko and R. G. Greaves, *Rad. Chem. and Phys.* **68**, 419, (2003).
26. J. R. Danielson, P. Schmidt, J. P. Sullivan, *et al.*, in *Non-Neutral Plasma Physics V*, edited by M. Schauer, T. Mitchell and R. Nebel (American Institute of Physics Press, Melville, NY, 2003), p. 149.